Original Article

Hypertensive Retinopathy Detection in Fundus Images Using Deep Learning-Based Model - Shallow ConvNet

Sina Garazhian [1], PhD; Alireza Meshkin [2,*], PhD

1 Department of Biotechnology, College of Sciences, University of Tehran, Tehran, Iran.
2 Department of Computer Engineering, Damavand Branch, Islamic Azad University, Damavand, Iran.

***Corresponding Author:** Alireza Meshkin
E-mail: a.meshkin@gmail.com

Abstract:

Background: Hypertensive Retinopathy (HR) is amongst the abnormalities occurred with high blood pressure. This high blood pressure level makes retinal arterial narrower, retinal hemorrhages and cotton wool spots more harmful. Based on what was mentioned, early detection of hypertensive retinopathy is pivotal to prevent its following disabilities and boost its treatment with more accurate methods.
Material and Methods: The main objective of this study is to investigate an appropriate deep learning method for improving the automatic diagnosis of hypertensive retinopathy in its early stages. The complete data used in this study have been obtained from integration of Structured Analysis of the Retina (STARE) and The Digital Retinal Images for Vessel Extraction (DRIVE) datasets.
Results: Interestingly, we reached an accuracy of 87.5 % after using the well-suited preprocessing method to integrate different images for further analysis by our designed convolutional neural network (CNN).
Conclusion: This model performs well with integration of two mentioned datasets.
Keywords: Hypertensive Retinopathy; Convolutional Neural Network; Deep Learning.

Article Notes: Received: Oct. 01, 2020; Received in revised form: Nov. 03, 2020; Accepted: Nov. 22, 2020; Available Online: Apr. 4, 2021.

How to cite this article: Garazhian S, Meshkin A. Hypertensive Retinopathy Detection in Fundus Images Using Deep Learning-Based Model - Shallow ConvNet. Journal of Ophthalmic and Optometric Sciences . 2021;5(2): 21-30.

Introduction

Hypertension is considered a widespread disease affecting the life of 9.4 million people [1] each year across the world, and it is expected to rise annually. Hypertension retinopathy disturbs retinal and blood vessels due to making blood pressure higher. Early detection of HR is necessary because it increases the possibility of cardiovascular and retina microcirculation. Mentioned diseases stemmed from HR observed in a lot of hypertensive cases. Vision loss [2] occurs when HR symptoms have begun. The fundus digital camera [3] can records microvascular changes. Nowadays, Fundus cameras are preferred because they are convenient and user-friendly. Hypertension originates from high arterial pressure; furthermore, it is the reason for most diseases around the world because it harms human tissues [4] and ultimately leads us to death [5] by cardiovascular diseases stemming from hypertensive retinopathy (HR).

Totally, irregularity originating from high blood pressure levels result in hypertensive retinopathy. Cotton wool spots (CWS) and retinal hemorrhage (HE), hemorrhages and microaneurysms (HM) are considered famous symptoms of HR [6]. A primitive diagnosis of HR-related eye diseases is a pivotal task [7] because mentioned diseases require early treatment to protect human life from its side effects. Conventionally, Ophthalmologists diagnose HR-related eye diseases with the help of fundus image analysis photographed by special cameras. The main objective of this study [8] is to design an intelligent diagnosis platform to help out ophthalmologists accurately interpret retinal fundus images in order to detect eye diseases caused by hypertensive retinopathy. several novel systems have been proposed for retinal image analysis in the previous articles, including the preprocessing of images for improved image quality, the segmentation of retinal HR-related areas and blood vessels as a step to extract features, and the classification of HR diseases with deep learning architectures [5]. Mainly, A pivotal sign of HR disease is uncommonly the wide veins make the ratio of average diameter to veins (AVR) lower; Thus, measuring the exact width of veins is too tricky for ophthalmologists.

Fundus image analysis through an automatic deep learning-based system highlights the vital point necessary for HR-related disease detection. To give a better illustration, these variation harms the HR-related regions and key eye areas. Thus, the inability to make an early diagnosis of mentioned variations causes severe hypertensive retinopathy (HR). The automated represented system is designed to help ophthalmologists for diagnosing HR-related diseases and their severity. The main aim of this kind of system is to assist medical care related occupations and researchers all over the world [9].

Few studies have stated the succession of hypertensive retinopathy detection (HR) by screening pivotal functional regions of the retina by segmentation approaches such as microaneurysms (MA), blood vessels (BV), optic disc (OD), and macula [6] as shown in figure 1. Deep learning models accurately extracted the mentioned structures. Then, the extracted features were utilized to detect abnormality anddeclare HR or non-HR disease. The related algorithms for extracting the full features for detecting HR-diseases are too heavy and complex, so researchers were striving to just extract the features more appropriately in contrast to the other essential indicators such as Hemorrhages or cotton wool spots. Finally, microaneurysms were discovered as an adequate marker for the early-

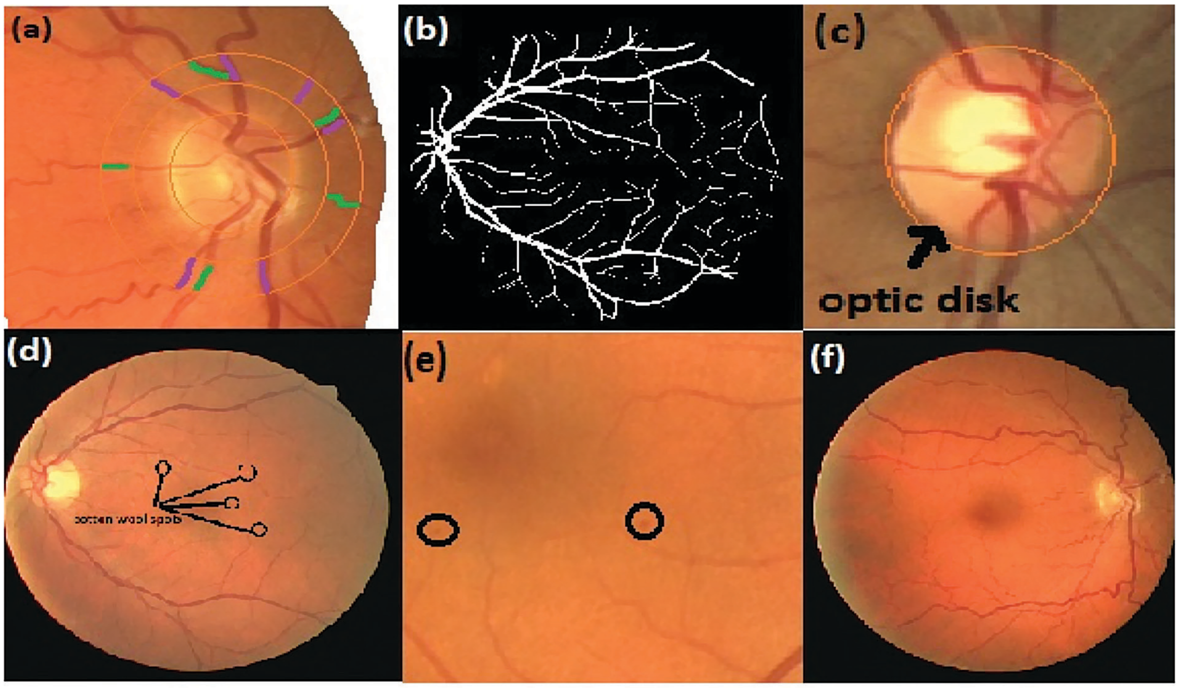

Figure 1: A graphical representation of (a) Arteriolar-to-venular (AV) ratio of diameters, (b) vessels of blood, (c) Optic disk (OD), (d) Cotton wool spot (CWS), (e) Microaneurysms (MA) and (f) Tortuosity and Hemorrhages (HM)

stage detection of hypertensive retinopathy, considering other injuries were required for diagnosing of malignant HR-related diseases.

Briefly, a new CNN architecture was utilized in this work with an innovative non-linear space transformation algorithm to make the images more uniform. Further, the accuracy metric besides sensitivity, precision, F1 score, and specificity was chosen to evaluate the model performance. Ultimately, the feasible future tasks were discussed to improve onset hypertensive retinopathy detection.

Convolutional Neural Network (CNN)

Interestingly, significant advances have been achieved in a majority of fields , including biology, medicine, sociology, etc., due to the recent development of deep learning (DL) [10-12]. The rudimentary principles of DL originate from artificial neural network (ANN) [13] research. It strives to model the hierarchical data representations and classify the ruling pattern by connecting the existing information layers to each other as a meaningful hierarchical structure. This sort of hierarchical learning is so robust due to its ability to learn complex patterns from large-sized input data. For instance, the input image is separated into a sequential vector form x = $^{1…xN}$ defined by equation (1) with the help of CNN model.

$$x_j^l = f\left(\sum_{i \in M_j} x^{l-1} * k_{ij}^l + b_j^l\right) \quad (1)$$

where x_j^l shows the jth output of the lth layer and * shows filter k has multiplied by the (l -1)th layer. Furthermore, f demonstrates the non-linear activation function, typically a rectified linear unit (f(x) = max(0,1)) (ReLu) and b_j demonstrates the bias part.

The first convolutional neural networks (CNNs) were developed in 1998 by Fukushima [14]. The deep learning approach has been applied in a wide range of areas, such as sentence classification [15], text recognition [16], face recognition [17], image characterization [18], object detection [19], pattern recognition [20], etc. A neuronal network consists of neurons with biases and weights that can be learned. It begins with an input layer, multiple hidden layers in the middle and ends up with an output layer. Each hidden layer made of a convolutional layer, pooling layer, fully connected layer (FC) and variety of normalization layers.

Convolutional layer

CNN's main building block is the convolutional layer, made of kernels (filters) and learnable parameters learned in the training process. Each kernel has responsibility for input image convolving and producing an activation map [21]. A kernel slides over the whole input image spatial positions, and the sum of elementwise multiplication between filters and the associated input image pixel is calculated at every pixel and put in an appropriate matrix as shown in figure 2.

Pooling layer

This layer is a dimension reduction non-linear tool working by connecting the output of the neuron cluster at one layer to the single neuron to help avoid overfitting and regulate the rotational variance of an input image. To give a better illustration, the pooling layer divides the input image into separate rectangular regions with values depending on the kind of pooling has chosen [22].

Fully connected layer (FC)

This CNN layer is put on next to the convolutional layer and the pooling layer. Each of its neurons has connected to the whole neuron of the previous layer as input connections with associated weights. Further, there is an output connection with weight equivalent to the sum of all the current neuron input weight multiplied by the corresponding weight. Its fundamental purpose is to act as a classifying operator.

Material and methods

Datasets

The designed ConvNet was evaluated via two prominent and publicly available fundus image datasets: STARE and DRIVE. The labels of the images were obtained based on ophthalmologist diagnosis to assess the proposed model in terms of accuracy, precision, sensitivity, F1 score and specificity.

Structured Analysis of Retina (STARE)

The STARE dataset [23] comprises 400 RGB fundus labeled images with various eye related abnormalities; the fundus images were photographed using a special fundus camera (TopCon TRV-50, Tokyo, Japan). The dataset is open to the public for related retinal image research with an image resolution of 605 × 700 pixels. Further, manual vessel segmentation is available for extra analysis. Totally, 40 images were chosen from the database, 30 normal images and 10 images introduce HR

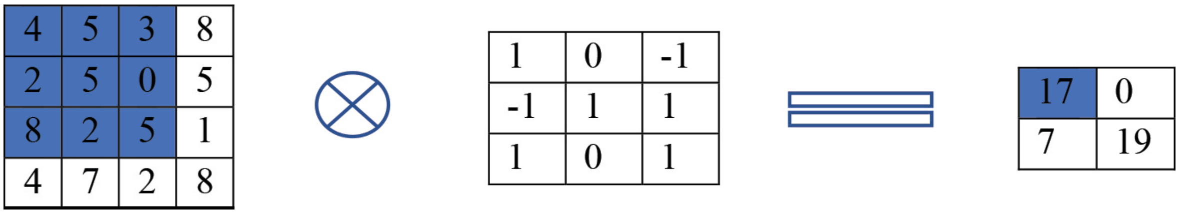

Figure 2: The Convolution process is illustrated graphically

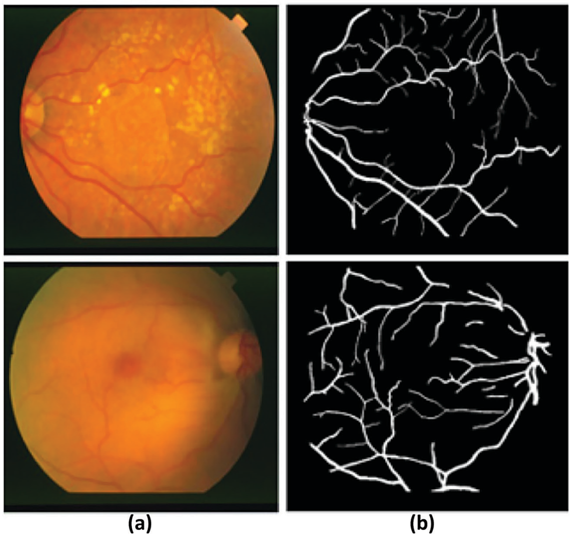

Figure 3: STARE dataset example images: (a) the original image used for input and (b) the mask of their related annotations

pathology. figure 3 illustrates sample images and their related vessel segmentation pairs.

DRIVE

The DRIVE dataset [24] comprises 40 images of fundus slides with annotations of various eye related abnormalities; the fundus images were photographed using a special fundus camera (Canon CR5 nonmydriatic 3CCD, New York, NY, USA). The dataset is available for public use with an image resolution of 565 × 584 pixels. In addition, manual vessel segmentation is available for further analysis. Whole 40 images were chosen from the database; 33 normal images and 7 images introduce the HR pathology. figure 4 illustrates sample images and their related vessel segmentation pairs.

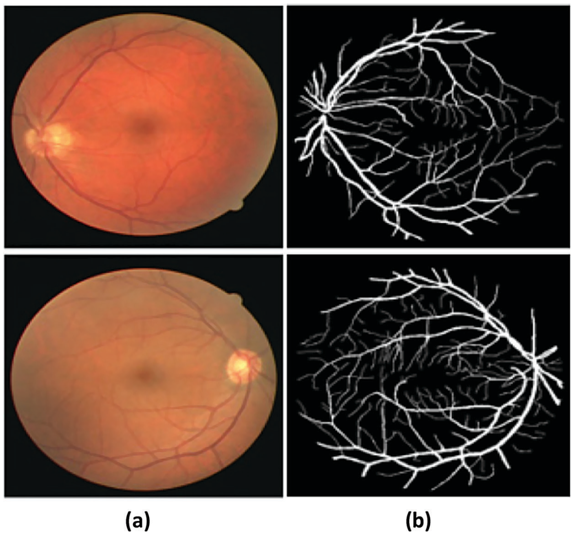

Figure 4: Images from the DRIVE dataset: (a) The original input image and (b) its associated annotation mask

method

Image preprocessing

A significant amount of information is lost due to gray scaling transformation because three pixel features convert to a single [6]. Furthermore, deletional information presented in an image is disregarded. Thus, in this paper, the nonlinear color transformation algorithm, CIEDE2000, on CIELAB color space is applied to create more uniform color spaces by applying the variation of color perceived by the human eye during the color transformation process [6]. Chroma and hue are represented by parameters A^* and B^*. Additionally, the difference between lightness and distance CIEDE2000 formula is shown by parameter L^* in CIELAB color space [6]. So, the CIELAB formula is given by Equation (2) as:

$$L^* = 116.f\left(\frac{Y}{Y_n}\right) - 166, b^* = 500\left[f\left(\frac{X}{X_n}\right) - f\left(\frac{Y}{Y_n}\right)\right], a^* = 200\left[f\left(\frac{Y}{Y_n}\right) - f\left(\frac{Z}{Z_n}\right)\right] \quad (2)$$

To support with better detail, The f parameter shows the nonlinearity function and the tristimulus values of the reference white color are X_n, Y_n, and Z_n.

Designed CNN

The Convolutional Neural Network (CNN) is implemented to help the task of hypertensive retinopathy (HR) Classification. Firstly, the input images were preprocessed for quality improvement to better classify input

Table 1: Parameters of the proposed model. The Number of Total parameters, trainable parameters and non-trainable parameters are 3075449, 3075281 and 168, respectively

Layer (type)	Output dimensions	Parameters number
Input layer	400*400*3	0
Convolution	199*199*64	1792
Batch normalization	199*199*64	256
Max pooling	49*49*64	0
dropout	49*49*64	0
flatten	153664	0
Fully connected	20	3073300
Batch normalization	20	80
dropout	20	0
Fully connected	1	21

images due to their highlighted regions in preprocessing step. Further, the images were resized to the resolution of 400 * 400 pixels. Secondly, the preprocessed images convert to matrix format as an input of CNN. Finally, the proposed deep learning model with the designed architecture was precisely trained until reaching a convergence, and the accuracy was calculated in each epoch of the classification process. figure 5 represents our proposed architecture, and table 1 shows our model parameters.

Related work

deep learning-based methods

A particular methodology of fundus image classification uses learning-based approaches. The mentioned methods are preferred as a result of a reduction in fundus preprocessing complexity. Various image processing tasks benefit from deep learning architecture, like feature extraction and segmentation without any preprocessing step.

A deep learning-based model was presented for HR detection [7]. 32*32 labeled grayscale fundus images were input of a deep learning model with final accuracy of 98.6 % for hypertensive retinopathy detection as an end goal. In [25], the variation of arterial blood vessels was assessed using a random Boltzmann machine (RBM) and a convolutional neural network (CNN) algorithm. The AVR ratio and OD region are selected features for the deep learning algorithms. In the mentioned research,

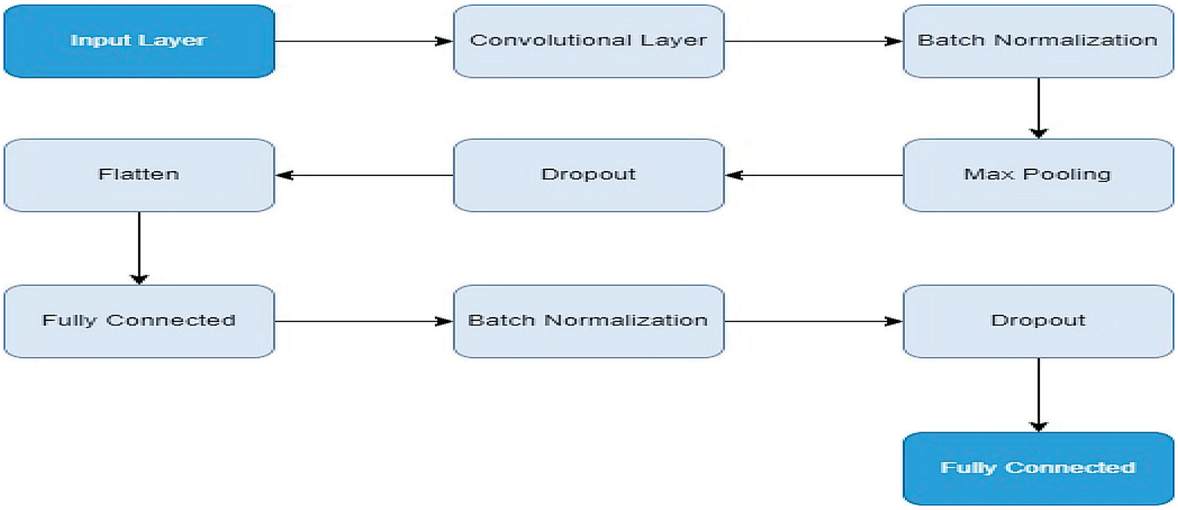

Figure 5: the flowchart representation of the designed CNN architecture

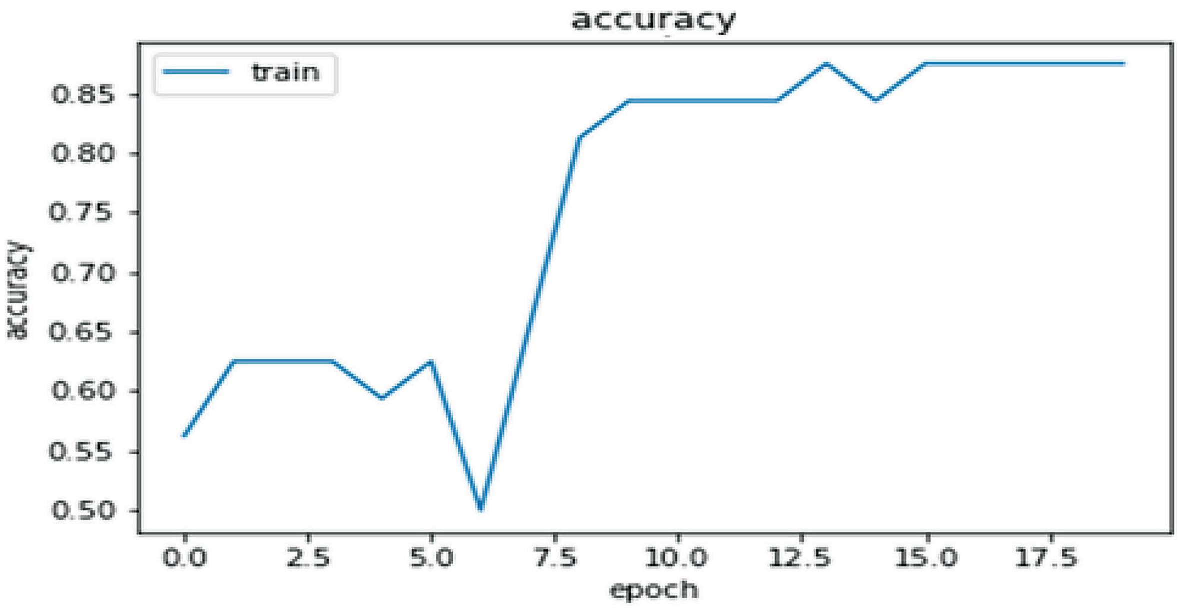

Figure 6: The accuracy of the proposed CNN architecture

a significantly higher accuracy was achieved. A CNN based approach to extract optic disc fovea centralis and retinal vessels was used [26]. The CNN architecture contains 7-layers and the output layer is made up of four nodes representing the optic disc, retinal vasculature, fovea centralis, and retinal background. A classification accuracy of 92.68 % was achieved using the DRIVE dataset. Also, The CNN architecture was used for segmentation and categorization of retinal vessels into arteries and veins [27, 28] in several studies. The mentioned approaches were determined with high accuracies for training with different databsets; 93.5 % for the DRIVE database and 88.89 % for a mediocre dataset of 100 fundus images. Ultimately, a CNN-based automatic machine to recognize exudates in microscopic retinograph was invented in [4]. The input data of the CNN was patches of unusual dimensions and preprocessed pixels positioned in the center of the patch. Convolutional layers are utilized to calculate probabilities of each pixel to be exudate or not. The proposed CNN contains four convolutional and pooling layers as hidden layers. The method was assessed with the help of the DRiDB dataset and had a F-score of 77 %.

Results and Discussion

The model was implemented in the python (3.7) to test and train the convolutional neural network with 16 and 64 images as test and train, respectively were obtained from integration of mentioned datasets. Based on experiment, an accuracy of 87.5 % is achieved for hypertensive retinopathy classification. This result can be due to the attempt to integrate two different datasets and issues with dimensions of images. So, this preprocessing method may be less appropriate for integrating of different datasets. However, there is not any comparison between other integration methods to make our study meaningful due to the lack of same research. figure 6 shows the accuracy graph of the learning process with 18 epochs.

Furthermore, the model was tested with the 5-fold cross validation approach to better evaluate its applicability in the real world, particularly in clinical images. At the end of each round of training, the hypertensive retinopathy probability of test dataset was predicted and integrated with following round results. Table 2 represents the confusion matrix of predicted capability of the trained model on the test dataset with related evaluation metrics. We measured the accuracy (ACC), specificity (SP), sensitivity (SE), precision (PR), and F1 score of the proposed model in order to evaluate its performance. These statistical metrics were used to assess the model performance by comparing the mentioned values with former developed models. We calculated the SE, SP, PR, F1 score, and ACC parameters using Equations [3, 7]. In order to calculate those statistics, the following equations were used. where TP, FN, TN, and FP are the numbers of true positives, false negatives, true negatives, and false positives, respectively. Here, TP is a picture that is recognized as a hypertensive retinopathy case in the test dataset and predicted as a hypertensive retinopathy case by our model, whereas FN is a picture that is recognized as a hypertensive retinopathy case in the test dataset but predicted by the model as a non-hypertensive retinopathy case. TN is a picture that is determined as a non-hypertensive retinopathy case and correctly predicted as a non-hypertensive retinopathy case by the model, whereas FP is a non-hypertensive picture in the test dataset and is predicted as a hypertensive retinopathy case by our model.

$$SE = \frac{\#TP}{\#TP+\#FN} \quad (3)$$

$$SP = \frac{\#TN}{\#TN+\#FP} \quad (4)$$

$$PR = \frac{\#TP}{\#TP+\#FP} \quad (5)$$

$$F1\ score = \frac{\#TP}{\#TP+0.5(\#FN+\#FP)} \quad (6)$$

$$ACC = \frac{\#TP+\#TN}{\#TP+\#TN+\#FP+\#FN} \quad (7)$$

Table 2: the whole dataset consists of 80 fundus images. Also, the train and test dataset had 64 and 16 images at each round, respectively

	Predicted Positive	Predicted Negative	
Actual Positive	51	1	Sensitivity = 0.98
Actual Negative	9	19	Specificity = 0.678
	Precision = 0.85	F1 score = 0.91	Accuracy = 0.875

There is a pivotal challenge when hypertensive retinopathy classification system was developed based on traditional methods. This mentioned issue is the lack of a large number of images in one unique dataset with the same image attributes. The ConvNet system is created in this paper to address the mentioned issue with the help of utilizing more complex preprocessing steps to integrate images of different datasets better and achieve a general system of hypertensive retinopathy classification.

Conclusion

Hypertensive Retinopathy is a vision-related abnormality that stems from the high blood pressure of eye veins. Thus, onset detection of HR is essential to stop its further side effects on eye which finally makes eye blind. This project aims to help HR diagnosis with deep learning algorithms to improve the accuracy of the mentioned process. Furthermore, the invented deep learning algorithm has the ability to rapidly detect HR by scanning the fundus image of eye with an accuracy of 87.5 % after preprocessing the input fundus image. The accuracy will be increased by using more complicated color space transformation-related algorithms will be invented in the near future due to rapid advance of knowledge.

Authors ORCIDs

Sina Garazhian:
https://orcid.org/0000-0003-3664-9939
Alireza Meshkin:
https://orcid.org/0000-0002-7046-4404

References

1. Writing Group M, Mozaffarian D, Benjamin EJ, Go AS, Arnett DK, Blaha MJ, et al. Executive Summary: Heart Disease and Stroke Statistics--2016 Update: A Report From the American Heart Association. Circulation. 2016;133(4):447-54.
2. Rosendorff C, Lackland DT, Allison M, Aronow WS, Black HR, Blumenthal RS, et al. Treatment of hypertension in patients with coronary artery disease: a scientific statement from the American Heart Association, American College of Cardiology, and American Society of Hypertension. Hypertension. 2015;65(6):1372-407.
3. Raghavendra U, Fujita H, Bhandary SV, Gudigar A, Tan JH, Acharya UR. Deep convolution neural network for accurate diagnosis of glaucoma using digital fundus images. Information Sciences. 2018;441:41-9.
4. Gamella-Pozuelo L, Fuentes-Calvo I, Gomez-Marcos MA, Recio-Rodriguez JI, Agudo-Conde C, Fernandez-Martin JL, et al. Plasma Cardiotrophin-1 as a Marker of Hypertension and Diabetes-Induced Target Organ Damage and Cardiovascular Risk. Medicine (Baltimore). 2015;94(30):e1218.
5. Wiharto, Suryani E. The review of computer aided diagnostic hypertensive retinopathy based on the retinal image processing. IOP Conference Series: Materials Science and Engineering. 2019;620(1):012099.
6. Abbas Q, Ibrahim MEA. DenseHyper: an automatic recognition system for detection of hypertensive retinopathy using dense features transform and deep-residual learning. Multimedia Tools and Applications. 2020;79(41):31595-623.
7. Triwijoyo BK, Pradipto YD. Detection of Hypertension Retinopathy Using Deep Learning and Boltzmann Machines. Journal of Physics: Conference Series. 2017;801:012039.
8. García-Floriano A, Ferreira-Santiago Á, Nieto OC, Yáñez-Márquez C. A machine learning approach to medical image classification: Detecting age-related macular degeneration in fundus images. Comput Electr Eng. 2019;75:218-29.
9. Asiri N, Hussain M, Al Adel F, Alzaidi N. Deep learning based computer-aided diagnosis systems for diabetic retinopathy: A survey. Artif Intell Med. 2019;99:101701.
10. Abbasi K, Razzaghi P, Poso A, Ghanbari-Ara S, Masoudi-Nejad A. Deep learning in drug target interaction prediction: current and future perspectives. Current Medicinal Chemistry. 2021;28(11):2100-13.
11. Hooshmand SA, Zarei Ghobadi M, Hooshmand SE, Azimzadeh Jamalkandi S, Alavi SM, Masoudi-Nejad A. A multimodal deep learning-based drug repurposing approach for treatment of COVID-19. Molecular diversity. 2021;25:1717-30.
12. LeCun Y, Bengio Y, Hinton G. Deep learning. Nature. 2015;521(7553):436-44.
13. Hong Z, editor A preliminary study on artificial neural network. 2011 6th IEEE Joint International Information Technology and Artificial Intelligence Conference; 2011 20-22 Aug. 2011.
14. Fukushima K. Neocognitron: A self-organizing neural network model for a mechanism of pattern recognition unaffected by shift in position. Biological Cybernetics. 1980;36(4):193-202.

15. Kim Y, editor Convolutional Neural Networks for Sentence Classification2014 October; Doha, Qatar: Association for Computational Linguistics.
16. Zhou X, Gong W, Fu W, Du F, editors. Application of deep learning in object detection. 2017 IEEE/ACIS 16th International Conference on Computer and Information Science (ICIS); 2017 24-26 .
17. Ranjan R, Sankaranarayanan S, Bansal A, Bodla N, Chen JC, Patel VM, et al. Deep Learning for Understanding Faces: Machines May Be Just as Good, or Better, than Humans. IEEE Signal Processing Magazine. 2018;35(1):66-83.
18. Druzhkov PN, Kustikova VD. A survey of deep learning methods and software tools for image classification and object detection. Pattern Recognition and Image Analysis. 2016;26(1):9-15.
19. Milyaev S, Laptev I. Towards reliable object detection in noisy images. Pattern Recognition and Image Analysis. 2017;27(4):713-22.
20. Patil A, Rane M, editors. Convolutional Neural Networks: An Overview and Its Applications in Pattern Recognition. Information and Communication Technology for Intelligent Systems; 2021 2021//; Singapore: Springer Singapore.
21. Mostafa S, Wu F-X. Diagnosis of autism spectrum disorder with convolutional autoencoder and structural MRI images. 2021. p. 23-38.
22. Sarvamangala DR, Kulkarni RV. Convolutional neural networks in medical image understanding: a survey. Evolutionary Intelligence. 2022;15(1):1-22.
23. Hoover AD, Kouznetsova V, Goldbaum M. Locating blood vessels in retinal images by piecewise threshold probing of a matched filter response. IEEE Transactions on Medical Imaging. 2000;19(3):203-10.
24. Staal J, Abramoff MD, Niemeijer M, Viergever MA, Ginneken Bv. Ridge-based vessel segmentation in color images of the retina. IEEE Transactions on Medical Imaging. 2004;23(4):501-9.
25. Chen C, Wei J, Peng C, Zhang W, Qin H. Improved Saliency Detection in RGB-D Images Using Two-Phase Depth Estimation and Selective Deep Fusion. IEEE Transactions on Image Processing. 2020;29:4296-307.
26. Deng J, Dong W, Socher R, Li LJ, Kai L, Li F-F, editors. ImageNet: A large-scale hierarchical image database. 2009 IEEE Conference on Computer Vision and Pattern Recognition; 2009 20-25 June 2009.
27. Akbar S, Akram MU, Sharif M, Tariq A, Yasin Uu. Arteriovenous ratio and papilledema based hybrid decision support system for detection and grading of hypertensive retinopathy. Computer Methods and Programs in Biomedicine. 2018;154:123-41.
28. Cavallari M, Stamile C, Umeton R, Calimeri F, Orzi F. Novel Method for Automated Analysis of Retinal Images: Results in Subjects with Hypertensive Retinopathy and CADASIL. Biomed Res Int. 2015;2015:752957.

Footnotes and Financial Disclosures

Conflict of interest:

The authors have no conflict of interest with the subject matter of the present manuscript.